IOSR Journal of Mathematics (IOSR-JM)
e-ISSN: 2278-0661,p-ISSN: 2278-8727, Volume 19, Issue 6, Ser. 1 (Nov. – Dec. 2023), PP 02-14
www.iosrjournals.org

Analysis Of Heat And Mass Transfer In Mhd Micropolar Jeffery Fluid Through A Porous Medium Over A Stretching Sheet

Ajay Nandan, Bhupander Singh*, Pravendra Kumar
Department of Mathematics, Meerut College (C.C.S University, Meerut), Meerut-250003, India

Abstract:
In the present paper we investigated the heat and mass transfer in the MHD micropolar Jeffery fluid flow over stretching sheet in the presence of porous medium. By using suitable similarity transformations, we get non-linear ordinary differential equations with the help of governing partial differential equations. We used DTM method for finding the analytical solution from the nonlinear ordinary differential equations. Obtained DTM solution is explored by bvp4c numerical solver built in MATLAB and effect of porosity parameter, Deborah number, magnetic field parameter, Jeffery fluid parameter etc. on velocity profile, temperature distribution, microrotation and concentration profile are explained by graphs. It is found that that as porosity parameter increases velocity decreases while increases in Prandtl number decreases the temperature profile distributions.

***Key words**: Micropolar fluid, Jeffery Fluid, MHD, Thermal Radiation, Porous Medium, Heat Transfer, Mass Transfer.*

Date of Submission: 24-10-2023 Date of Acceptance: 04-11-2023

I. Introduction:

Now a days the micropolar fluid has vast applications in various aspects (fields) of science and engineering technology. Eringen [1,2] introduces the theory of micropolar fluids. Wilson [3] investigated the basic flows of micropolar fluid. A spin vorticity relation for unidirectional plane flows is studied by Kilne [4]. Gorla [5] and Adnan [6] analyzed the flows along the horizontal and vertical axes. Crane [7] studied the flow of an ambient fluid over a sheet (linear stretching) for the two-dimensional steady problem and found a correspondence solution in the form of a closed analytical. Ariman et al. [8] analyzed micropolar and thermos-micropolar fluid in engineering and technology. Fully convective flow in a vertical channel for micropolar viscous fluid was investigated by Prathap Kumar et al. [9]. Srinivasacharya et al. [10] investigated the unsteady flow of micropolar fluid between two parallel porous plates. The mixed convection flow of micropolar fluid with uniform suction driven by a porous stretching sheet using a finite element method (FEM) is presented by Bhargava et al. [11].

The boundary layer flow, Heat and mass transfer in a stagnant Newtonian and non-Newtonian fluid driven by a continuous stretching sheet are of relevance in a large number of engineering processes in industry such as the drawing of filaments or a polymer sheet extruded consistently from a die, metallic plate's cooling in a bath, the aerodynamic extraction of plastic sheets, the continuous rolling casting, thinning and annealing of copper wires, fiber coating and wires etc. The final obtained product of desirable characteristics depends upon the cooling's and stretching's process. Mohammadi and Nourazar [12] investigated the insertion of a gas layer which was very thin in micro cylindrical couette flows containing power law liquids. The analytical solution between two rotating cylinders filled with a gas of micro layer and power-law liquid for two phase flow has been studied by Mohammadi et al. [13]. Gupta and Gupta [14] analyzed the effect of transfer of Heat_Mass on a stretching sheet along with blowing or suction. Apart from these different aspects for the problem have been analyzed by Chen and Char [15] and Dutta et al. [16]. Hina et al. [17] Investigated the impact of heat and mass transfer on the MHD peristaltic flow of a Maxwell fluid in a planer channel with compliant walls. In a permeable channel the effect of heat transfer of micropolar fluid was analyzed by M. Sheikholeslami et al. [18]. A. Mirzaaghaian and D.D. Ganji [19] got the DTM solution through permeable walls for micropolar fluid with heat transfer. P. Sibanda et al. [20] studied about the flow for a micropolar fluid with the transfer of heat and mass through a channel. Also, some boundary value problems for the flow of micropolar fluid was analyzed by Bhupander Singh [21-23].

It is very well known that commonly the industrial fluids are different from viscous fluids because of diverse rheological characteristics. These fluids belong to the category of non-Newtonian fluids and have different applications like wire and blade coating, dying of, paper and textile plastics manufacturing, polymer industries, geophysics, food processing, petroleum and chemical processes. Materials like apple sauce, soaps, foams, drilling muds, sugar solution pastes, clay coating, ketchup, lubricant, certain oils, suspension and colloidal solutions are the non-Newtonian liquids movement of biological fluids and many others. The normal Navier-stokes equations are unable to characterize the behavior of the flow of non-Newtonian liquids. No one relationship is capable of predicting the properties of all non-Newtonian materials. As a result, many non-Newtonian model types are offered in the literature. The present study is about the Jeffery fluid. A rate-type substance called Jeffery fluid exhibits the fluid's linear viscoelastic effect. There are several uses of Jeffery fluid in the polymer industry. Jeffery fluid can have several forms, one of which is diluted polymer solution. Generally, Jeffery fluid is complicated direct model to utilize time derivative in place of convected derivative and utilized by most fluid models. Jeffery fluid model is implemented for depicting the qualities of relaxation times and retardation. Hayat et al. [24] have studied about the series solutions for MHD flow of Jeffery fluid through a porous channel by using homotopy analysis method. Using long wavelength and low Reynolds number approximations, Srinivas and Muthuraj [25] have examined the issue of MHD peristaltic transport of a Jeffery fluid in an inclined asymmetric channel under the impact of slip condition at the channel wall. Eldabe et el. [26] used the perturbation approach for a small geometric parameter to examine the impact of wall attributes on the peristaltic transport of a dusty fluid with heat_mass transfer. According to long wavelength and Low Reynolds number assumptions, Vajravelu et al. [27] explored the peristaltic flow of a Jeffery fluid in a vertical porous stratum with heat transmission. In a channel with slip effect at a lower wall, Aruna Kumari et al. [28] explored the impact of heat transfer on MHD oscillatory flow of Jeffery fluid. The formulas for the velocity and temperature are determined analytically. The MHD flow of a Jeffrey fluid in convergent and divergent channels is examined by Asadullah et al [29]. Physical and biological sciences heavily rely on fluxes between no parallel barriers. In a horizontal channel with chemical reaction, Idowa et al. [30] investigated the impact of heat_mass transfer on unstable MHD oscillatory flow of Jeffery fluid. In a channel with a porous medium, Adesanya and Makinde [31] investigated MHD oscillatory slip flow and heat transfer. Al-Khafajy [32] examines how heat affects the body. A.M. Abd-Alla et al. [33] studied impact of heat-mass transfer in a rotating frame for a Jeffery fluid in presence of chemical reactions. Wall properties are also taken in consideration. Kottakkaran Sooppy Nisar et al. [34] found semi analytical solutions of Jeffery fluid flow in presence of chemical reaction and heat source.

Fig. 1 Graph for the problem:

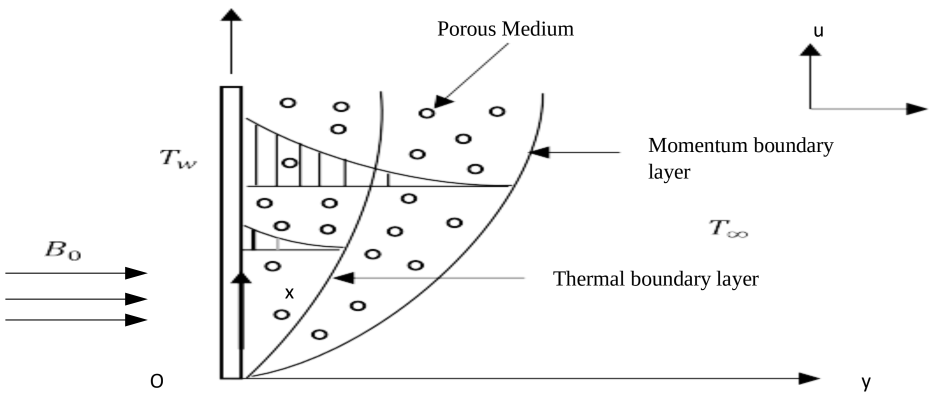

II. Mathematical Formulation

Let us considered a two-dimensional incompressible Jeffrey micropolar fluid flow across a stretched sheet that coincides with the plane $y = 0$ and the flow is contained within the plane with y > 0. It is expected that the surface will extend linearly at a speed $u = u_w = ax$, where a is the stretching constant. The coordinates (x, y) in this case are selected such that the x-axis is parallel to the vertical surface and the y-axis is normal to it. In addition, (u, v) are the flow's velocity components, and N designates the internal speed of the micropolar particles. The unit of gravity is g. The sheet is subjected to B_0, uniform magnetic field that is applied normally. Heat and mass transfer also taken into consideration. The Jeffery fluid equations are written as:

$\tau = -pI + S$, and $S = \frac{\mu}{(1+\lambda_1)}\left[R_1 + \lambda_2\left(\frac{\partial R_1}{\partial t} + V.\nabla\right)R_1\right]$,

Where, Cauchy stress tensor is denoted by τ while extra stress tensor is denoted by S, λ_1 and λ_2 are material parameters of Jeffery fluid, Rivlin Ericksen tensor is defined by $R_1 = (\nabla V) + (\nabla V)^t$, μ represents dynamic viscosity.

Now, Equations for the problem are given as:

$$\frac{\partial u}{\partial x} + \frac{\partial v}{\partial y} = 0 \tag{1}$$

$$u\frac{\partial u}{\partial x} + v\frac{\partial u}{\partial y} = \frac{\nu}{1+\lambda_1}\left(1+\frac{k}{\mu}\right)\left[\frac{\partial^2 u}{\partial y^2} + \lambda_2\left(u\frac{\partial^3 u}{\partial x \partial y^2} + v\frac{\partial^3 u}{\partial y^3} + \frac{\partial u}{\partial y}\frac{\partial^2 u}{\partial x \partial y} - \frac{\partial u}{\partial x}\frac{\partial^2 u}{\partial y^2}\right)\right] - \frac{\sigma B_0^2 u}{\rho} + \frac{k}{\rho}\frac{\partial N}{\partial y} + g\beta_T(T - T_\infty) + g\beta_C(C - C_\infty) \tag{2}$$

$$u\frac{\partial T}{\partial x}+v\frac{\partial T}{\partial y}=\frac{k}{\rho c_p}\frac{\partial^2 T}{\partial y^2}-\frac{1}{\rho c_p}\frac{\partial q_r}{\partial y} \quad (3)$$

$$u\frac{\partial N}{\partial x}+v\frac{\partial N}{\partial y}=\frac{\gamma}{\rho j}\frac{\partial^2 N}{\partial y^2}-\frac{k}{\rho j}\left(2N+\frac{\partial u}{\partial y}\right) \quad (4)$$

$$u\frac{\partial C}{\partial x}+v\frac{\partial C}{\partial y}=D\frac{\partial^2 C}{\partial y^2} \quad (5)$$

The appropriate boundary conditions for the problem are given by

$$\left.\begin{array}{l} u=u_w=ax,\; v=0, N=-n\frac{\partial u}{\partial y}, T=T_w \text{ at } y=0 \\ u\to 0, N\to 0, T\to T_\infty \text{ at } y\to\infty \end{array}\right\}, \quad (6)$$

where u and v are velocity components along the x-axis and y-axis respectively, ρ is the fluid density, N is the angular or micro rotation velocity, λ_1 is relaxation ratio while λ_2 is relaxation time, T is the fluid temperature and c_p is the specific heat at constant pressure, k is the thermal conductivity and j is the micro-inertia density, β_T is coefficient of thermal expansion and β_C is coefficient of concentration expansion, D = diffusion coefficient. n is boundary concentration parameter of fluid., the case n = 0 represents strong concentration, n = 0.5 indicates weak concentration.

Now, Under Rosseland diffusion approximation the Thermal radiation is simulated and in accordance with this, q_r the radiative heat flux is given by:

$$q_r=-\frac{4\sigma^*}{3\sigma k^*}\frac{\partial T^4}{\partial y}$$

(7a)

where $\sigma^*$is the Stefan–Boltzmann constant and k^* is the Rosseland mean absorption coefficient. If the temperature differences are sufficiently small, then by expanding T^4 into the Taylor's series about T_∞ and neglecting higher order terms, we get $T^4=4T_\infty^3 T-3T_\infty^4$

and then

$$\frac{\partial q_r}{\partial y}=-\frac{16\sigma^* T_\infty^3}{3\sigma k^*}\frac{\partial^2 T}{\partial y^2}$$

(7b)

We now introduce the following Similarities variables:

$$u=ax\frac{\partial f}{\partial\eta},\; \eta=\sqrt{\frac{a}{\upsilon}}\,y,\; v=-\sqrt{(a\upsilon)}\,x\,f(\eta),\; N=a\sqrt{\frac{a}{\upsilon}}\,g(\eta),\; \theta(\eta)=\frac{T-T_\infty}{T_w-T_\infty}$$

(8)

By using equations (6) – (8), equations (2) – (5) transformed in to the equations:

$$(1+A)f'''(\eta)+(1+\lambda)\left[\left\{\left(f'(\eta)\right)^2-\left(f(\eta)f''(\eta)\right)\right\}-\left(M+K_p\right)f'(\eta)+Ag'(\eta)+G_r\theta+G_c\phi\right]+(1+A)\beta\left[\left\{\left(f''(\eta)\right)^2-\left(f(\eta)f^{iv}(\eta)\right)\right\}\right]=0 \quad (9)$$

$$\left(1+\frac{4}{3}R\right)\theta''(\eta)+P_r f(\eta)\theta'(\eta)=0 \quad (10)$$

$$\left(1+\frac{A}{2}\right)g''(\eta)+f(\eta)g'(\eta)-g(\eta)f'(\eta)-A\left(2g(\eta)+f''(\eta)\right)=0$$

(11)

$$\frac{D}{\nu}\phi''(\eta)+f(\eta)\phi'(\eta)=0 \quad (12)$$

Boundary conditions (6) in similarity variables become

$$\left.\begin{array}{l} f(0)=0, f'(0)=0, g(0)=-nf''(0), \theta(0)=1, \phi(0)=1 \\ f'(\eta)\to 0, g(\eta)\to\infty, \theta(\eta)\to\infty(0), \phi(\eta)=1 \; as\; \eta\to\infty \end{array}\right\}$$

(13)

Where $A=\frac{k}{\mu}$, (Micropolar Parameter), $M=\frac{\sigma B_0{}^2}{\rho a}$, (Magnetic Parameter), $K_P=\frac{\mu}{\rho a k_1}$, (Porosity Parameter),

$P_r=\frac{\mu C_P}{\kappa}$, (Prandtl Number), $R=\frac{4\sigma^* T_\infty^3}{3\kappa k^*}$, (Radiation Parameter), $E_c=\frac{a^2x^2}{C_P(T_w-T_\infty)}$, (Eckert Number) $\beta=\lambda_2 a$(Deborah number) , $G_r=\frac{g\beta_T(T_w-T_\infty)}{a^2x}$ (Grashhof number for Heat transfer),

$G_c=\frac{g^*\beta_c(C_w-C_\infty)}{a^2x}$ (Grashhof number for mass transfer) , $\frac{D}{\nu}=S_c$ (Schmidt number)

Also, skin friction, Nusselt numbers and Sherwood numbers are defined as:

$C_f = \frac{2T_w}{\rho U_w^2}$, $N_u = \frac{q_w}{T_w - T_\infty}\left(\frac{x}{K}\right)$ and $S_h = \frac{q_m}{D(C_w - C_\infty)}$
(14)

Where $T_w = -\frac{\nu}{1+\lambda_1}\left[\frac{\partial u}{\partial y} + \lambda_2\left(u\frac{\partial^2 u}{\partial x \partial y} + v\frac{\partial^2 u}{\partial y^2}\right) + \left(\frac{k}{\mu}\right)N\right]_{y=0}$ $q_w = -\left(\frac{\partial T}{\partial y}\right)_{y=0}$ and $q_w = -D\left(\frac{\partial C}{\partial y}\right)_{y=0}$ (15)

By using similarity conditions, we get:

$Re_x^{1/2} C_f = \frac{1}{1+\lambda_1}\left(f''(0) + \beta f''(0)\right)$, $N_u Re_x^{-1/2} = -\theta'(0)\left(1 + \frac{4}{3}R\right)$, $S_h Re_x^{-1/2} = -\phi'(0)$
(16)

III. Method of solution

Fundamentals of DTM (differential transformation method) [27] are explored as follows:

Differential transformation of the k^{th}derivative of a function $f(\eta)$ is defined as

$$F(k) = \frac{1}{k!}\left[\frac{d^k f(\eta)}{d\eta^k}\right]_{\eta=\eta_0}$$
(17)

Where F(**k**) is called the T function of $f(\eta)$ at $\eta = \eta_0$ in k-domain.
The differential inverse transformation of F(**k**) is defined as

$$f(\eta) = \sum_{k=0}^{\infty} F(k)\,(\eta - \eta_0)^k$$
(18)

By combining Equation (17) and Equation (18), f(η) can be obtained as

$$f(\eta) = \sum_{k=0}^{\infty}\left[\frac{d^k f(\eta)}{d\eta^k}\right]_{\eta=\eta_0}\frac{1}{k!}(\eta - \eta_0)^k$$
(19)

In practice, to achieve a finite one, this infinite series truncated as follows

$$f(\eta) = \sum_{k=0}^{N} F(k)\,(\eta - \eta_0)^k$$
(20)

Theorems to be used in transformation procedure, can be evaluated from equations (17)-(18), are given in table 1.

Table 1: Some basics operations of DTM

Original Function	Transformed Function
$f(\eta) = \alpha g(\eta) \pm \beta h(\eta)$	$F[k] = \alpha G[k] + \beta H[k]$
$f(\eta) = \frac{d^n f(\eta)}{df(\eta)}$	$F[k] = \frac{(k+\eta)!}{k!}G[(k+\eta)]$
$f(\eta) = g(\eta)h(\eta)$	$F(k) = \sum_{m=0}^{k} F(m)H(k-m)$
$f(\eta) = e^{m\eta}$	$F(k) = \frac{m^k}{k!}$
$f(\eta) = (1+\eta)^m$	$F(k) = \frac{(m)(m-1)\dots\dots\dots(m-k+1)}{k!}$
$f(\eta) = (\eta)^m$	$F(k) = \delta(k-m) = \begin{Bmatrix} 1, & k=m \\ 0, & k \neq m \end{Bmatrix}$
$f(\eta) = sin(\omega\eta + \alpha)$	$F(k) = \frac{\omega^k}{k!}sin\left(\frac{\pi k}{2} + \alpha\right)$
$f(\eta) = cos(\omega\eta + \alpha)$	$F(k) = \frac{\omega^k}{k!}cos\left(\frac{\pi k}{2} + \alpha\right)$

Now we will find DTM Solution of the problem so applying differential transformation method to (9) - (12), we obtained:

$$(1+A)(K+1)(K+2)(K+3)F[K+3] + (1+\lambda)[\sum_{m=0}^{K}\{F[K-m].(m+1)(m+2)F[m+2] + (M+K_P)(K+1)F(K+1) + A(K+1)G(K+1) + G_r(K+1)\theta(K+1) + G_C(K+1)\phi(K+1)] + (1+A)\beta[\sum_{m=0}^{K}(K-m+2)(K-m+1)F[K-m+2].(m+1)(m+2)F[m+2] - \sum_{m=0}^{K}(K-m+1)F[K-m+1].(m+1)(m+2)(m+3)(m+4)F[m+4]] = 0$$
(21)

$$\left(1+\frac{4}{3}R\right)(K+1)(K+2)\theta[K+2] + P_r[\sum_{m=0}^{K}F[K-m].(m+1)\theta[m+1]] = 0.$$
(22)

$\left(1+\frac{A}{2}\right)(\mathrm{K}+1)(\mathrm{K}+2)\mathrm{G}[\mathrm{K}+2]+\ [\sum_{\mathrm{m}=0}^{\mathrm{K}}\mathrm{F}[\mathrm{K}-\mathrm{m}]\,.\,(\mathrm{m}+1)\ \mathrm{G}[\mathrm{m}+1]]-[\sum_{\mathrm{m}=0}^{\mathrm{K}}\mathrm{G}[\mathrm{K}-\mathrm{m}]\,.\,(\mathrm{m}+1)\ \mathrm{F}[\mathrm{m}+1]]-A[2\ \mathrm{G}[\mathrm{K}]+(\mathrm{K}+1)\ (\mathrm{K}+2)\ \mathrm{F}(\mathrm{K}+2)]=0.$ (23)

$\frac{D}{\nu}(\mathrm{K}+1)(\mathrm{K}+2)\phi[\mathrm{K}+2]+[\sum_{\mathrm{m}=0}^{\mathrm{K}}\mathrm{F}[\mathrm{K}-\mathrm{m}].(\mathrm{m}+1)\ \phi[\mathrm{m}+1]]=0$ (24)

With boundary conditions:

$F[0]=0,\ F[1]=1,\ F[2]=\alpha_1.$ (25a)

$G[0]=-2n\alpha_1,\ G[1]=\alpha_2,\ \theta[1]=\alpha_{3,}\ \phi[1]=\alpha_{4,}$ (25b)

At infinity DTM is not possible. So, Pade approximation will be applied to find the value of coefficients $\alpha_1,\ \alpha_2$ and α_3 as a result the Pade coefficients $\alpha_1=0.226552,\ \alpha_2=0.584349, \alpha_3=0.835702\ and\ \alpha_4=0.758397$ are substituted into the Equations (21)-(24), therefore, the expressions of $f(\eta), g(\eta), \theta(\eta)\ and\ \varphi(\eta)$ can be obtained in case of $\mathrm{A}=1.0,\ \mathrm{P_r}=2.0,\ \mathrm{G_c}=0.8, \mathrm{G_r}=0.7, \mathrm{M}=2.5\ \ \beta=0.3,\ \mathrm{K_p}=0.5\ , \eta=0.5, \mathrm{R}=1.5, \lambda_1=0.6, \mathrm{S_c}=0.6$ as:

$f(\eta)=\eta+(0.226552\ )\eta^2+\ (-0.021458883)\eta^3+\ (-0.007193689\ )\eta^4+(-0.019994244\ )\eta^5+\ (-0.002776511)\eta^6+\ (0.009348757)\eta^7+(-0.001923854)\eta^8+(-0.000194596)\eta^9+\ldots\ldots\ldots$ (26)

$g(\eta)=(-0.226552\ )+\ (0.584349\ )\ \eta+(-0.075509782)\eta^2+\ (0.104165638)\eta^3+(-0.000808365)\eta^4+\ (-0.013948162)\eta^5+\ (-0.001911567\ )\eta^6+(0.006016452)\eta^7+(-0.001329722)\eta^8+\ (-0.0000370873)\eta^9+\ldots$ (27)

$\theta(\eta)=1+\ (0.835702)\ \eta+\ (-0.092846492)\eta^3+\ (-0.010602478\ )\eta^4+\ (0.005193903)\eta^5+(0.002478341)\eta^6+\ (-0.000089355)\eta^7+\ (-0.00025413)\eta^8+\ (-0.000146973)\eta^9+\ldots\ldots\ldots\ldots\ldots\ldots$ (28)

$\phi(\eta)=1+\ (0.758397)\ \eta+\ (-0.0758397)\eta^3+\ (-0.008590818\ )\eta^4+(0.011865387)\eta^5+(0.001827277)\eta^6+\ (-0.000589437)\eta^7+(-0.00026435)\eta^8+\ (-0.000074758)\eta^9+\ldots\ldots\ldots$ (29)

IV. Graphical Result and discussion:

The objective of this study is to analyze the heat and mass transfer in MHD micropolar Jeffery fluid in a porous medium over a stretching sheet. In this section we discuss the effect of various parameters like Porosity parameter, Deborah number, magnetic field parameter, Jeffery fluid parameter, Grashoff number for mass transfer and Grashoff number for heat transfer on the velocity profile, microrotation, temperature distribution and concentration profile.

In Fig. 2 we see the effect of porosity parameter (i.e. $\mathrm{K_p}=0.5, 1.5, 2.5$) on velocity profile with the values $\mathrm{A}=1.0,\ \mathrm{P_r}=2.0,\ \mathrm{G_c}=0.8, \mathrm{G_r}=0.7, \mathrm{M}=2.5\ \ \beta=0.3, \eta=0.5, \mathrm{R}=1.5, \lambda=0.6, S_c=0.6$ as and we observe that as porosity parameter increases velocity profile decreases.

Also In Fig. 3 we analyze the Deborah number's effect (i.e. $\beta=0.3, 0.6, 1.0$) on velocity profile with the values $\mathrm{A}=1.0,\ \mathrm{P_r}=2.0,\ \mathrm{G_c}=0.8, \mathrm{G_r}=0.7, \mathrm{M}=2.5,\ \mathrm{K_p}=0.5\ , \eta=0.5, \mathrm{R}=1.5, \lambda_1=0.6, S_c=0.6$ and we find that as Deborah parameter increases velocity decreases. Fig. 4 shows the behavior of velocity profile corresponding to magnetic field parameter (i.e. M = 2.5, 4.0, 6.0) with the values $\mathrm{A}=1.0,\ \mathrm{P_r}=2.0,\ \mathrm{G_c}=0.8, \mathrm{G_r}=0.7, \mathrm{K_p}=0.5\ , \eta=0.5, \mathrm{R}=1.5, \lambda=0.6, S_c=0.6$ and we observe that as magnetic field parameter increases velocity decreases. Fig. 5 depicts the effect of Jeffery fluid parameter (i.e., $\lambda=0.4, 0.6, 0.8$)on velocity profile corresponding to the values $\mathrm{A}=1.0,\ \mathrm{P_r}=2.0,\ \mathrm{G_c}=0.8, \mathrm{G_r}=0.7, \mathrm{M}=2.5,\ \mathrm{K_p}=0.5\ , \eta=0.5, \mathrm{R}=1.5, S_c=0.6$ and we see that velocity decreases as Jeffery fluid parameter increases.

Fig.2. Simulated velocity for various values of porosity parameter

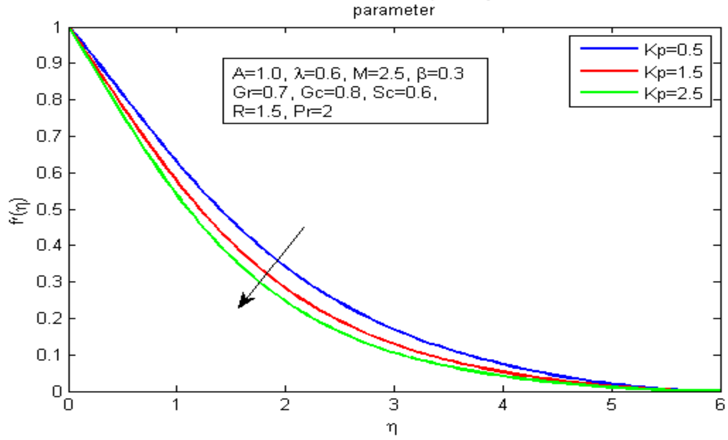

Fig.3. Simulated velocity profile for various values of Deborah number

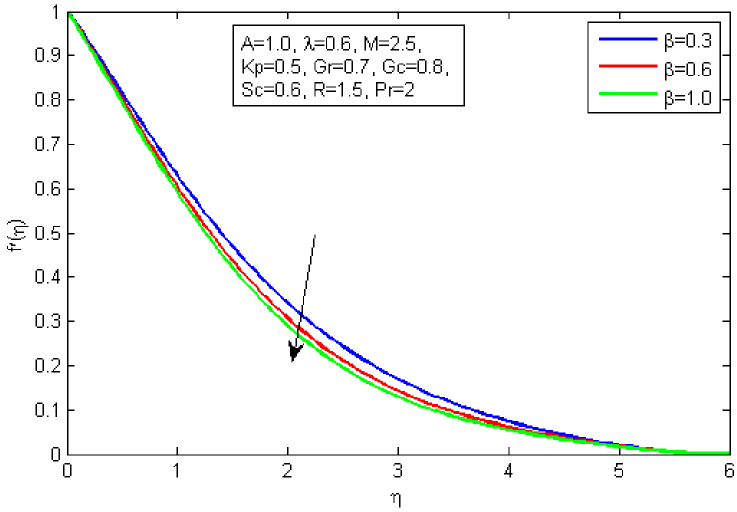

Fig.4. Simulated velocity for various values of magnetic field parameter

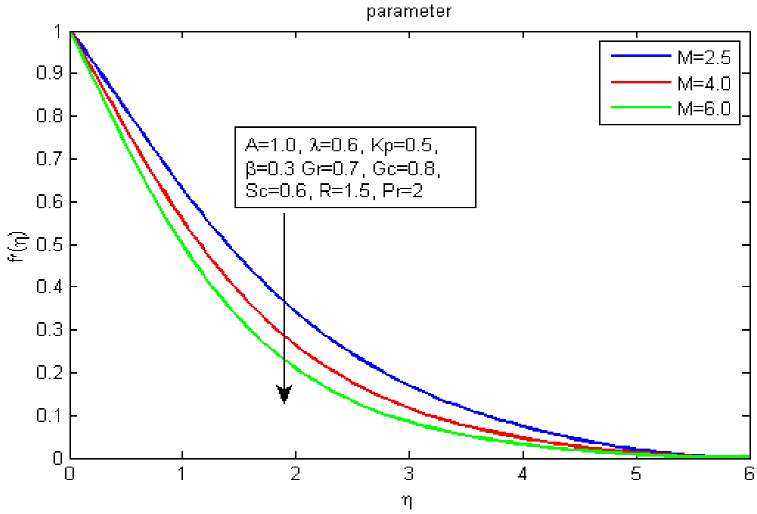

Fig.5. Simulated velocity for various values of Jeffrey fluid parameter

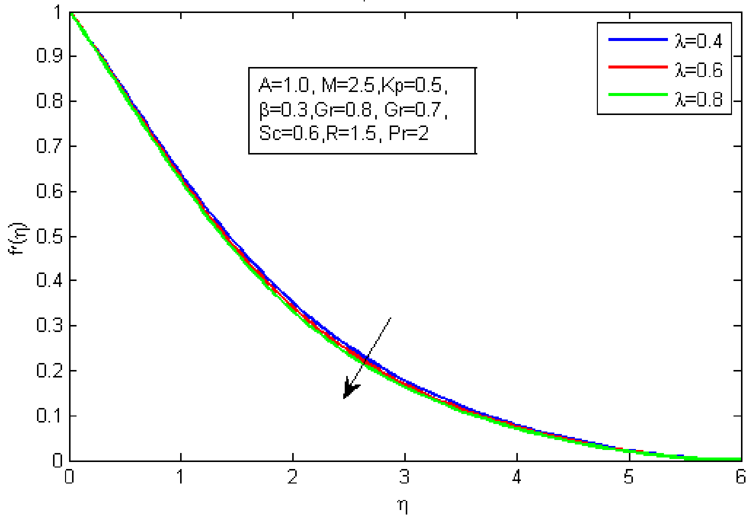

Fig.6. Simulated velocity for various values of Gr

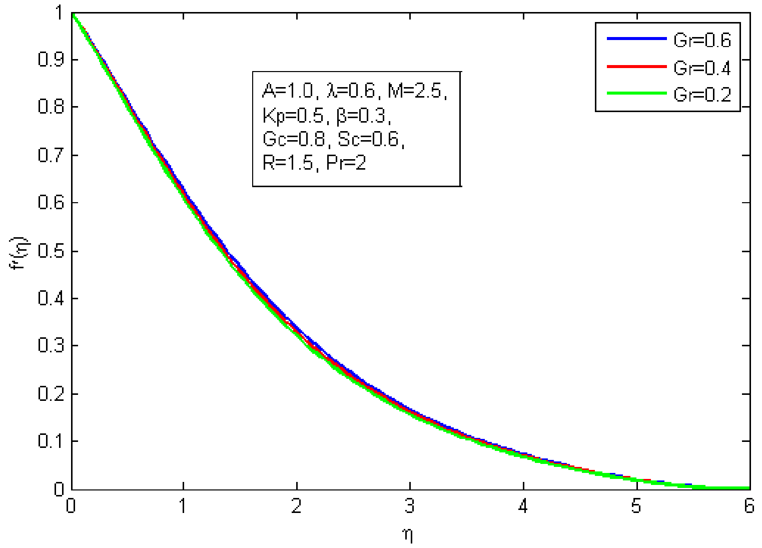

Fig.7. Simulated velocity for various values of Gc

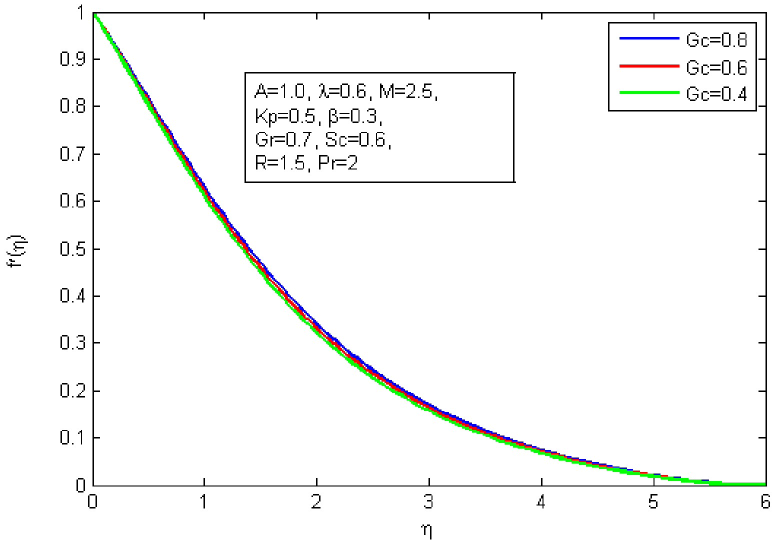

Fig.8.Simulated Velocity Profile for different values of micropolar parameter

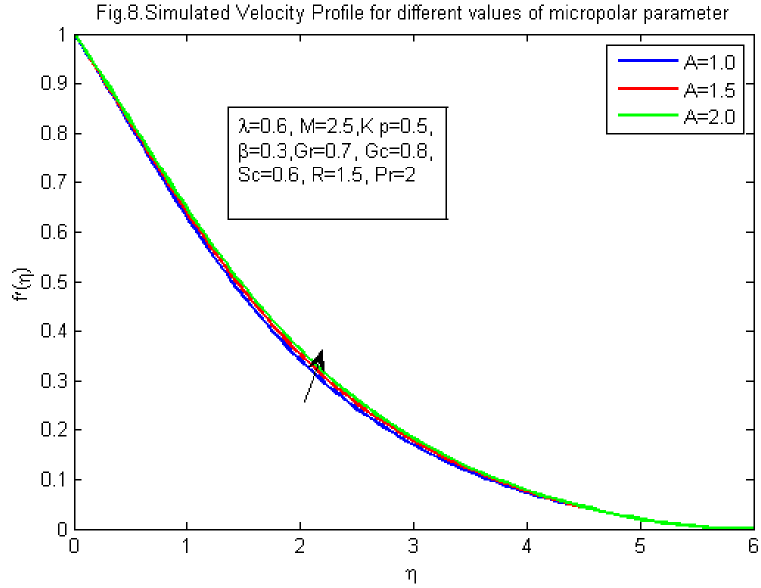

Fig.9. Microrotation for different values of micropolar parameter

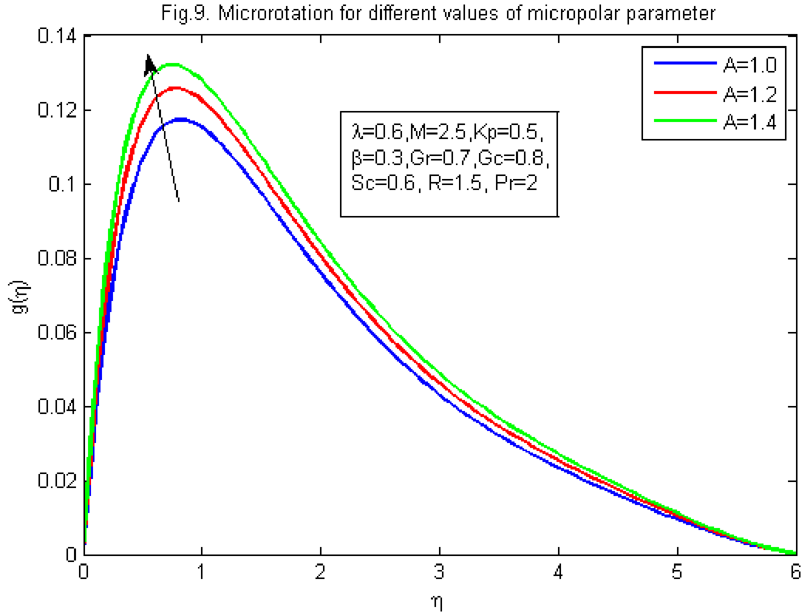

It is shown in Fig. 6 and Fig. 7 that velocity decreases as Gr and Gc increases with the values $A = 1.0, P_r = 2.0, M = 2.5, K_p = 0.5, \eta = 0.5, R = 1.5, \lambda = 0.6, S_c = 0.6$. Fig. 8 shows the depict effect of micropolar parameter on velocity profile corresponding to the values $P_r = 2.0, G_c = 0.8, G_r = 0.7, M = 2.5, K_p = 0.5, \eta = 0.5, R = 1.5, \lambda = 0.6, S_c = 0.6$ and we observe that as micropolar parameter increases velocity also increases. Fig. 9 and Fig. 10 represents the behavior of microrotation for the micropolar parameter and magnetic field parameter for the values of different parameters and with the behavior of figures we conclude that as micropolar parameter increases microrotation also increases while as the magnetic field parameter increases microrotation decreases.

Fig.10. Microrotation for different values of magnetic parameter

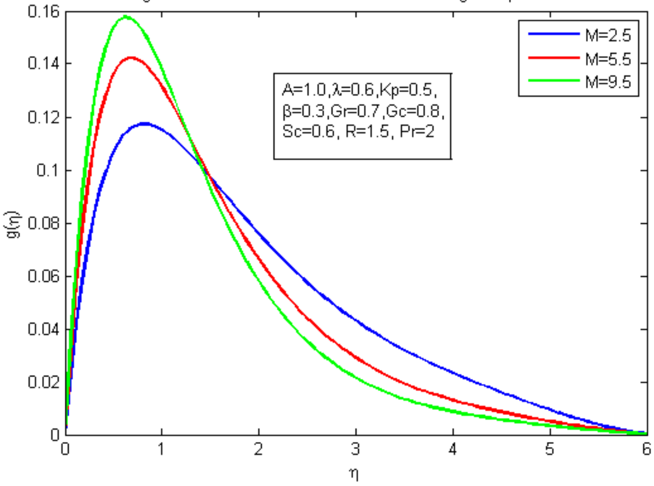

Fig.11. Temperature distributions for different values of Prandtl number

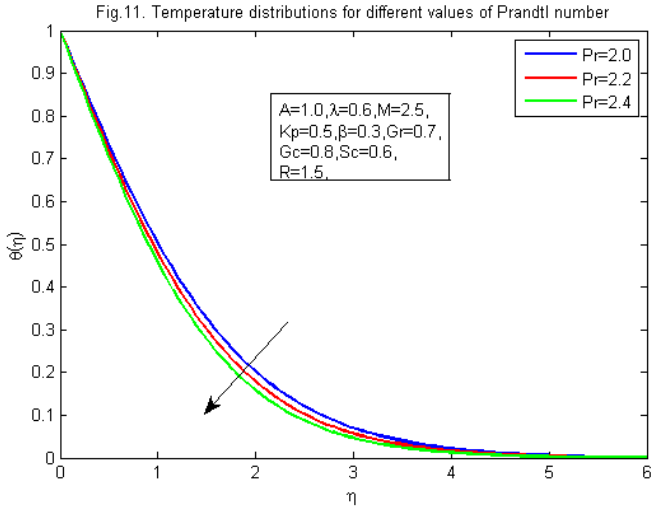

Fig.12. Temperature distributions for different values of radiation parameter

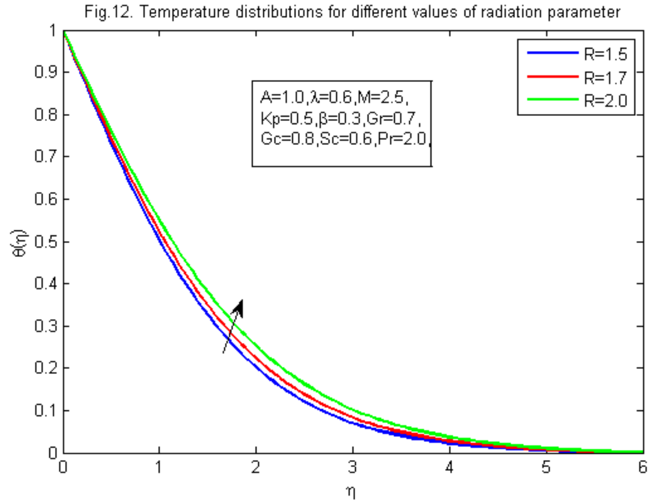

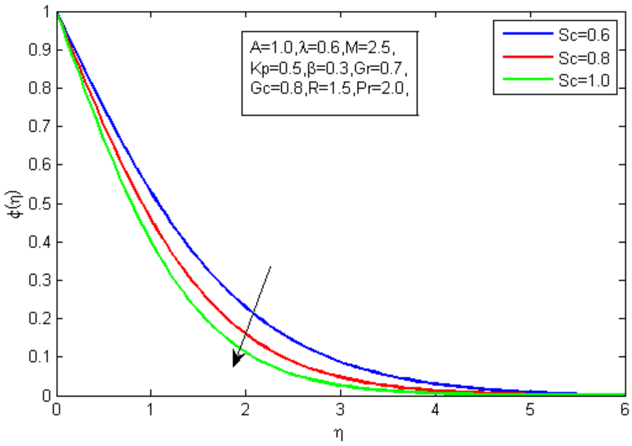

In Fig. 11 we see the effect of different values of Prandtl number on temperature distribution with the values $A = 1.0$, $G_c = 0.8, G_r = 0.7, M = 2.5$, $K_p = 0.5$, $\eta = 0.5, R = 1.5, \lambda = 0.6, S_c = 0.6$ and we observe that as temperature distribution decreases as Prandtl number increases. Fig. 12 depicts the effect of different values of radiation number on temperature distribution for the values $A = 1.0$, $P_r = 2.0$, $G_c = 0.8, G_r = 0.7, M = 2.5$, $K_p = 0.5$, $\eta = 0.5, \lambda = 0.6, S_c = 0.6$ and we find that temperature distribution increases as radiation number increases. In Fig. 13 we see the effect of different values of Schmidt number on concentration profile with the values $A = 1.0$, $P_r = 2.0$, $G_c = 0.8, G_r = 0.7, M = 2.5$, $K_p = 0.5$, $\eta = 0.5, R = 1.5, \lambda = 0.6$, and we observe that Concentration profile increases as Schdmit number increases

We also discussed the effect of various parameters on C_f N_u and S_h and represented the results tabular form.

Table 2: Effects of various parameters on C_f

uS.NO.	A	λ	Sc	Gr	-f"(0)	$Re_x^{1/2} C_f = \frac{1}{1+\lambda_1}\left(f''(0) + \beta f''(0)\right)$
1	1.1	0.6	0.6	0.7	0.3274	0.266013
2	1.3	0.6	0.6	0.7	0.334	0.271375
3	1.5	0.6	0.6	0.7	0.3376	0.2743
4	1.7	0.6	0.6	0.7	0.3444	0.279825
5	1	0.6	0.6	0.7	0.3235	0.262844
6	1	0.8	0.6	0.7	0.3123	0.253744
7	1	1	0.6	0.7	0.3007	0.244319
8	1	1.2	0.6	0.7	0.2889	0.234731
9	1	0.6	0.8	0.7	0.3239	0.263169
10	1	0.6	1	0.7	0.3243	0.263494
11	1	0.6	1.2	0.7	0.3246	0.263738
12	1	0.6	1.4	0.7	0.325	0.264063
13	1	0.6	0.6	0.9	0.3175	0.257969
14	1	0.6	0.6	1.1	0.3114	0.253013
15	1	0.6	0.6	1.3	0.3053	0.248056
16	1	0.6	0.6	1.5	0.2979	0.242044

Table 2 shows the effect of micropolar parameter, Jeffery fluid parameter, schmidt number and Grashoff number for heat transfer on skin friction and we observe that as skin friction increases as micropolar parameter and schmidt number increases and decreases as Jeffery fluid parameter and Grashoff number for heat transfer decreases.

Table 3: Effects of various parameters on N_u :

S.NO.	R	λ	P_r	Gr	Gc	$\theta'(0)$	$= -\theta'(0)\left(1+\frac{4}{3}R\right)$
1	1.7	0.6	2	0.7	0.8	-0.4031	1.2093
2	1.9	0.6	2	0.7	0.8	-0.3975	1.1925
3	2.1	0.6	2	0.7	0.8	-0.3928	1.1784
4	2.3	0.6	2	0.7	0.8	-0.3887	1.1661
5	1.5	0.6	2	0.7	0.8	-0.4097	1.2291
6	1.5	0.8	2	0.7	0.8	-0.4099	1.2297
7	1.5	1	2	0.7	0.8	-0.4102	1.2306
8	1.5	1.2	2	0.7	0.8	-0.4105	1.2315
9	1.5	0.6	2.2	0.7	0.8	-0.4178	1.2534
10	1.5	0.6	2.4	0.7	0.8	-0.4261	1.2783
11	1.5	0.6	2.6	0.7	0.8	-0.4345	1.3035
12	1.5	0.6	2.8	0.7	0.8	-0.443	1.329
13	1.5	0.6	2	0.9	0.8	-0.4098	1.2294
14	1.5	0.6	2	1.1	0.8	-0.4099	1.2297
15	1.5	0.6	2	1.3	0.8	-0.4101	1.2303
16	1.5	0.6	2	1.5	0.8	-0.4117	1.2351
17	1.5	0.6	2	0.7	1	-0.4098	1.2294
18	1.5	0.6	2	0.7	1.2	-0.4099	1.2297
19	1.5	0.6	2	0.7	1.4	-0.4101	1.2303
20	1.5	0.6	2	0.7	1.6	-0.4117	1.2351

Table 3 shows the effect of radiation parameter, Jeffery fluid parameter, Prandtl number, Grashoff number for mass transfer and Grashoff number for heat transfer on Nusselt number and we observe that as Nusselt number increases as Jeffery fluid parameter, Prandtl number, Grashoff number for mass transfer and Grashoff number for heat transfer increases and decreases as radiation parameter decreases.

Table 4: Effects of various parameters on S_h

S.NO.	λ	Sc	Gr	Gc	$-\phi'(0)$
1	0.6	0.6	0.7	0.8	0.4016
2	0.8	0.6	0.7	0.8	0.4018
3	1	0.6	0.7	0.8	0.4021
4	1.2	0.6	0.7	0.8	0.4024
5	0.6	0.8	0.7	0.8	0.4261
6	0.6	1	0.7	0.8	0.4515
7	0.6	1.2	0.7	0.8	0.4778
8	0.6	1.4	0.7	0.8	0.5048
9	0.6	0.6	0.9	0.8	0.4017
10	0.6	0.6	1.1	0.8	0.4018
11	0.6	0.6	1.3	0.8	0.402
12	0.6	0.6	1.5	0.8	0.4034
13	0.6	0.6	0.7	1	0.4017
14	0.6	0.6	0.7	1.2	0.4018
15	0.6	0.6	0.7	1.4	0.402
16	0.6	0.6	0.7	1.6	0.4034

Table 4 shows the effect of Jeffery fluid parameter, schmidt number, Grashoff number for mass transfer and Grashoff number for heat transfer on Sherwood number and we observe that as Sherwood number increases as Jeffery fluid parameter, schmidt number, Grashoff number for mass transfer and Grashoff number for heat transfer increases.

V. Conclusions:

We have the following conclusion from the graphs:

- Velocity profile decreases as the different parameters like porosity parameter, Deborah number, magnetic field parameter, Jeffery fluid parameter, Gr, Gc decreases.
- Velocity profile decreases as the micropolar parameter increases.
- Increases in Prandtl number decreases in temperature profile distributions.
- Concentration profile increases as Schmidt number increases.
- Microrotation increases as micropolar parameter increases.
- Skin friction increases as micropolar parameter and schmidt number increases
- Skin friction decreases as Jeffery fluid parameter and Grashoff number for heat transfer decreases.
- Nusselt number increases as Jeffery fluid parameter, Prandtl number, Grashoff number for mass transfer
- Nusselt number decreases Grashoff number for heat transfer increases and decreases as radiation parameter decreases.
- Sherwood number increases as Jeffery fluid parameter increases.
- Sherwood number increases schmidt number increases.
- Sherwood number increases Grashoff number for mass transfer and Grashoff number for heat transfer increases.

References:

[1]. Eringen, A.C., Simple micropolar fluid, Int. J. Engg. Sci., 2, 205-217 (1964).
[2]. Eringen, A.C., Theory of micropolar fluids, J. Math. Mech., 16, 1-18 (1966).
[3]. Wilson, A.J., Basic flows of micropolar fluids, Appl. Sci. Res., 20, 338-355 (1969).
[4]. Kilne, K.A., A spin vorticity relation for unidirectional plane flows of micropolar fluids, Int. J. Engg. Sci., 15, 131-134 (1977).
[5]. Gorla, R.S.R. and Takhar, H. S., Free convection boundary layer flow of a micropolar fluid past a cylinder bodies, Int. J. Engg. Sci., 25, 949-962 (1987).
[6]. Adnan Y., Mixed convection in micropolar fluid flow over a horizontal plate with surface mass transfer, Int. J. Engg. Sci., 27, 1593-1602 (1989).
[7]. Crane LJ. Flow past a stretching plate. Z Angew Math Phys; 21:645–647 (1970)
[8]. T. Ariman, M.A. Turk, N.D. Sylvester, Microcontinuum fluid mechanics-a review, Int. J. Eng. Sci. 11, 905–930, (1973)
[9]. J. Prathap Kumar, J.C. Umavathi, Ali J. Chamkha, I. Pop, fully developed free convective flow of micropolar and viscous fluids in a vertical channel, Appl. Math. Model. 34, 1175–1186, (2010)
[10]. D. Srinivasacharya, J.V. Ramana murthy, D. Venugopalam, unsteady stokes flow of micropolar fluid between two parallel porous plates, Int. J. Eng. Sci. 39, 1557–1563, (2001)
[11]. R. Bhargava, L. Kumar, H.S. Takhar, Finite element solution of mixed convection micropolar fluid driven by a porous stretching sheet, Int. J. Eng. Sci. 41, 2161–2178, (2003)
[12]. M.R. Mohammadi, S.S. Nourazar, On the insertion of a thin gas layer in micro cylindrical Couette flows involving power-law liquids, Int. J. Heat Mass Transf. 75, 97–108 (2014).
[13]. M.R. Mohammadi, S.S. Nourazar, A. Campo, Analytical solution for two-phase flow between two rotating cylinders filled with power-law liquid and a micro layer of gas, J. Mech. Sci. Technol. 28 (5), 1849–1854 (2014).
[14]. P.S. Gupta, A.S. Gupta, Heat and mass transfer on a stretching sheet with suction or blowing, Can. J. Chem. Eng. 55 (1977),744–746 (1977).
[15]. C.K. Chen, M.I. Char, Heat transfer of a continuous stretching surface with suction or blowing, J. Math. Anal. Appl. 135, 568–580 (1988).
[16]. B.K. Datta, P. Roy, A.S. Gupta, Temperature field in the flow over a stretching sheet with uniform heat flux, Int. Common., Heat Mass Transf. 12, 89–94 (1985).
[17]. S. Hina, T. Hayat and A. Alsaedi, Heat and mass transfer effects on the peristaltic flow of Johnson-Segalman fluid in a curved channel with compliant walls, Int. J Heat Mass Transfer., 55, 3511-3521 (2012).
[18]. Sheikholeslami, M.; Hatami, M.; Ganji, D.D.G.-D. Micropolar fluid flow and heat transfer in a permeable channel using analytical method. J. Mol. Liq.,194, 30–36 (2014).
[19]. Mirzaaghaian, A., Ganji, D. Application of differential transformation method in micropolar fluid flow and heat transfer through permeable walls. Alex. Eng. J., 55, 2183–2191 (2014).
[20]. Sibanda, P., Awad, F. Flow of a micropolar fluid in channel with heat and mass transfer. In Proceedings of the 2010 International Conference on Theoretical and Applied Mechanics, International Conference on Fluid Mechanics and Heat & Mass Transfer, Corfu Island, Greece, 22–24, 112–120, (2010).
[21]. Singh, B. Thermal convection of MHD micropolar fluid layer heated from below saturating a porous medium. IOSR J. Eng. (IOSR-JEN), 8, 45–52 (2018).
[22]. Singh, B. Hall effect on MHD flow of visco-elastic micro-polar fluid layer heated from below saturating a porous medium. Int. J. Eng. Sci. Technol., 9, 48–66 (2017).
[23]. Singh, B. Thermal instability of a rotating MHD micropolar fluid layer heated from below saturating a porous medium. Int. J. Pure Appl. Math., 118, 1393–1405 (2018).
[24]. T. Hayat, R. Sajjad, S. Asghar, Series solution for MHD channel flow of a Jeffery fluid, Commun Nonlinear Sci Numer Simulat., 15, 2400–2406 (2010).
[25]. S. Srinivas and R. Muthuraj, Peristaltic transport of a Jeffrey fluid under the effect of slip in an inclined asymmetric channel, Int. J Appl. Mech. 2, 437–455 (2010).
[26]. N. T. Eldabe, K. A. Kamel, G. M. Abd- Allah and S.F. Ramadan, Peristaltic motion with Heat and Mass transfer of a Dusty fluid through a Horizontal porous channel under the effect of wall properties, Int. J Research Reviews in Appl. Sciences., 15 300- 311 (2013).

[27]. K. Vajravelu S. Sreenadh, P. Lakshminarayana, The influence of heat transfer on peristaltic transport of a Jeffrey fluid in a vertical porous stratum, Commun Nonlinear Sci Numer Simulat., 16, 3107-3125 (2011).

[28]. Aruna Kumari B., Ramakrishna Prasad K. and Kavita K., Slip Effects on MHD Oscillatory Flow of Jeffrey Fluid in a Channel with Heat Transfer. International Journal of Mathematics Arch. 3 (8), 2903 – 2911 (2012).

[29]. Asadullah M., Umar K., Nareed A., Raheela M. and Mohyud – Din S.T. MHD Flow of a Jeffrey Fluid in Converging and Diverging Channels. International Journal of Mathematics science. 6 (2), 92 – 106 (2013).

[30]. Idowu, A.S, Joseph, K.M and Daniel, S. Effect of Heat and Mass Transfer on Unsteady MHD Oscillatory Flow of Jeffrey Fluid in a Horizontal Channel with Chemical Reaction. Journal of Mathematics (IOSR-JM), 8(5), 74-87 (2013).

[31]. Adesanya, S.O and Makinde, O.D. MHD Oscillatory slip flow and heat transfer in channel filled with porous media. U.P.B. Science Bull. Series A, 76 (1) (2014).

[32]. Al-khafajy, D.G.S Effects of heat transfer on MHD oscillatory flow of Jeffrey fluid with variable viscosity through porous medium. Advances in Applied Science Research, 7(3), 179-186 (2016).

[33]. A.M. Abd-Alla, S.M. Abo-Dahab, Esraa N. Thabet, F.S. Bayones and M.A. Abdelhafez Heat and mass transfer in a peristaltic rotating frame Jeffrey fluid via porous medium with chemical reaction and wall properties. Alexandria Engineering Journal 66, 405–420 (2023).

[34]. Kottakkaran Sooppy Nisar, R. Mohapatra, S.R. Mishra, and M. Ganeswar Reddy Semi-analytical solution of MHD free convective Jeffrey fluid flow in the presence of heat source and chemical reaction. Ain Shams Engineering Journal 12, 837–845 (2023).